Lithuanian Journal of Physics, Vol. **62**, No. 4, pp. 221–228 (2022)

PHOSPHATE BONDED $CoFe_2O_4$–$BaTiO_3$ LAYERED STRUCTURES: DIELECTRIC RELAXATIONS AND MAGNETOELECTRIC COUPLING

A. Plyushch [a], D. Lewin [b], P. Ažubalis [a], V. Kalendra [a], A. Sokal [c], R. Grigalaitis [a], V.V. Shvartsman [b], S. Salamon [d], H. Wende [d], A. Selskis [e], K.N. Lapko [c], D.C. Lupascu [b], and J. Banys [a]

[a] *Faculty of Physics, Vilnius University, Saulėtekio 9, 10222 Vilnius, Lithuania*
[b] *Institute for Materials Science and Center for Nanointegration Duisburg-Essen (CENIDE), University of Duisburg-Essen, Universitätsstraße 15, 45141 Essen, Germany*
[c] *Affiliation-independent researchers*
[d] *Faculty of Physics and Center for Nanointegration Duisburg-Essen (CENIDE), University of Duisburg-Essen, Lotharstraße 1, 47057 Duisburg, Germany*
[e] *Department of Structural Analysis of Materials, Center for Physical Sciences and Technology, Saulėtekio 3, 10257 Vilnius, Lithuania*
Email: artyom.plyushch@ff.vu.lt

Received 14 October 2022; accepted 18 October 2022

Multilayered phosphate bonded $CoFe_2O_4$–$BaTiO_3$–$CoFe_2O_4$ (CBC) and $BaTiO_3$–$CoFe_2O_4$ – $BaTiO_3$ (BCB) multiferroic structures were formed by means of uniaxial pressing. The dielectric properties were studied in 20 Hz – 1 GHz frequency and 120–500 K temperature ranges. The complex dielectric permittivity is 15–0.17i for CBC and 22–0.04i for BCB, it is temperature- and frequency-independent below 250 K. At higher temperatures, strong dispersion appeared governed by the Maxwell–Wagner relaxation. Such behaviour is determined by the 2–2 connectivity of the sample. The highest direct magnetoelectric coupling coefficient was found for the $BaTiO_3$–$CoFe_2O_4$–$BaTiO_3$ structure of 0.2 $mVOe^{-1}cm^{-1}$.

Keywords: phosphate bonded ceramics, barium titanate, cobalt ferrite, layered structures, Maxwell–Wagner relaxation, multiferroics, magnetoelectrics, magnetoelectric coupling

1. Introduction

Multiferroics are single- or multi-phase materials that demonstrate more than one ferroic order: ferroelastic, ferromagnetic or ferroelectric. Magnetoelectric (ME) composites comprising piezoelectric and ferrite phases exhibit unique properties, in particular, the coupling effect between the components allows one to polarize samples with an external magnetic field and vice versa.

According to different spatial distributions of phases or connectivity, composites are divided into several groups. The whole variety of connectivities is not limited to only 0–3 and 2–2 [1, 2]; however, the most studied are the two mentioned. The 0-3 type composites are particulate composites with high sintering temperatures. Due to this, some unpredictable phases are produced easily at the interfaces. As a result, the performance of the 0–3 composites degrades [3, 4]. Layered composites possess higher values of the magnetoelectric response in comparison to those of bulk ME materials [5–8]. Yang et al. demonstrated that the magnetoelectric coupling coefficient of layered 2–2 structures is four times larger than that of the bulk ones [7]. Together with that, the 2–2 structures offer a wider range of preparation techniques: bonding of previously sintered layers [9], tape casting [10, 11], chemical

solution deposition [12], sputtering and physical vapour deposition [13]. Any of the mentioned methods have pros and cons: casted structures induce inner mechanical stresses upon annealing due to shrinkage mismatch [14], bonded with polymer tablets [9] degrade at higher temperatures due to the degradation of epoxy, deposition techniques are time and resource consuming.

Previously, it has been demonstrated that phosphate bonding is a promising approach for the preparation of composite bulk 0–3 magnetoelectric ceramics. It provides a combination of the simplicity of the preparation procedure with a relatively high coupling coefficient [15]. Samples are uniaxially pressed, which means that such an approach may be applied for the 2–2 connectivity.

This research aims to synthesize the layered $BaTiO_3$ and $CoFe_2O_4$ structures, using a phosphate bonding of powders, into a ceramic material. The impact of the 2–2 connectivity on the dielectric properties and magnetoelectric coupling coefficient is measured and discussed.

2. Materials and methods

An aluminium phosphate binder (APB) was synthesized by the dissolution method. At the first step, an aqueous suspension of aluminium hydroxide $Al(OH)_3$ was prepared. Then a concentrated solution (85 wt.%) of orthophosphoric acid was added in portions to $Al(OH)_3$ dispersion under continuous stirring and heating of the reaction mixture up to 363–373 K for 2.5–3 h until a viscous transparent solution was obtained. The molar ratio of H_3PO_4 and $Al(OH)_3$ was equal to 3:1. Being prepared, the obtained transparent solution of APB was diluted with distilled water to a density of 1.42 g/cm^3.

Commercially available $BaTiO_3$ (*Sigma-Aldrich*, 208108, grain size <3 μm, designated as BTO) and $CoFe_2O_4$ (*Sigma-Aldrich*, 773352, mean grain size of 30 nm, designated as CFO) powders were used for the preparation of the multilayer phosphate bonded structures. Two different mixtures of barium titanate with diluted $Al(H_2PO_4)_3$ and cobalt ferrite with the binder were prepared separately by carefully grinding the components in an agate mortar for 10–15 min. The content of the binder in both mixtures was 5 wt.%. The prepared mixtures were used to form a layered structure. On each step, an amount of 0.1 g BTO/APB or CFO/APB mixture was poured into a pressing mould and the plain surface was levelled by manually pressing. After the 3-layer structure was formed it was pressed into tablets of 1 cm in diameter under 6 tons. As a result, layered tablets $CoFe_2O_4$–$BaTiO_3$–$CoFe_2O_4$ and $BaTiO_3$–$CoFe_2O_4$–$BaTiO_3$ were prepared (see Fig. 1). Further in the text, the samples are labelled as CBC and BCB, respectively. The average thickness of a single layer is 0.3 mm, and the total thickness is 0.9–0.91 mm.

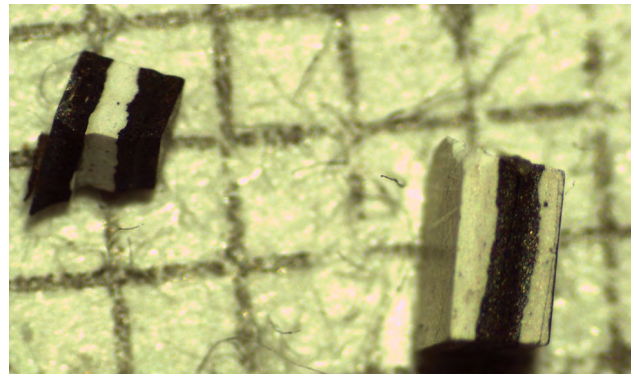

Fig. 1. Optical microscopy of the layered structures. The background is millimetre paper.

Scanning electron microscopy was performed with a Helios NanoLab 650 microscope. The broadband dielectric spectra were investigated in a frequency range of 20 Hz – 1 GHz. For the quasi-static range up to 1 MHz, an LCR HP4284A was used. In a frequency range of 1 MHz – 1 GHz, ε was studied with a coaxial line spectrometer with a vector network analyzer *Agilent* 8714ET. For both frequency ranges, custom-made heaters and liquid nitrogen cryostats were used for temperature measurements. The temperature was measured with a *Keithley* 2700 multimeter. The measurements were done on cooling with a rate of 1 K/min. The samples with an area of 2–3 mm^2 were prepared for measurements. Silver paste was applied as an electric contact.

The direct magnetoelectric coupling coefficient was measured with a custom-made set-up [16] based on the dynamic lock-in detection technique [17]. The polarized sample (5 kV/cm) was placed in the system of four electromagnets with the configuration of the magnetic field of $H = H_0 + H_{ac}$. Bruker electromagnets were used to generate the static field $\mu_0 H_0$ in a range of –1 to 1 T. A low amplitude $\mu_0 H_{ac}$

field was generated with Helmholtz coils connected to an ac source (*Brul and Kjaer*, Naerum, Denmark). Both magnetic fields were applied in parallel. The ME-induced voltage was measured by a lock-in amplifier SR830. Silver electrodes were sputtered to as-prepared pellets for measurements.

3. Results and discussion

Scanning electron microscopy of the CBC sample is presented in Fig. 2(a). Bigger grains on the right correspond to the BTO/APB layer, and CFO/APB is on the left. According to the EDX mapping (Fig. 2(b)), the interface is clear, interpenetrations were not detected.

3.1. Dielectric properties

Temperature dependences of the real and imaginary parts of dielectric permittivity are presented in Fig. 3. Below 250 K, both samples demonstrate frequency- and temperature-independent dielectric permittivity of 15–0.17i and 22–0.04i for CBC and BCB, respectively. Above 250 K, a strong frequency dispersion is observed in the real part accompanied by frequency-dependent pronounced maxima in ε''. At higher temperatures, the dielectric permittivity of CBC is twice higher than the one of BCB and reaches 700. The dielectric losses of CBC are 3 times higher in comparison with those of BCB, up to 250 at peak. In contrast to the bulk samples [15],

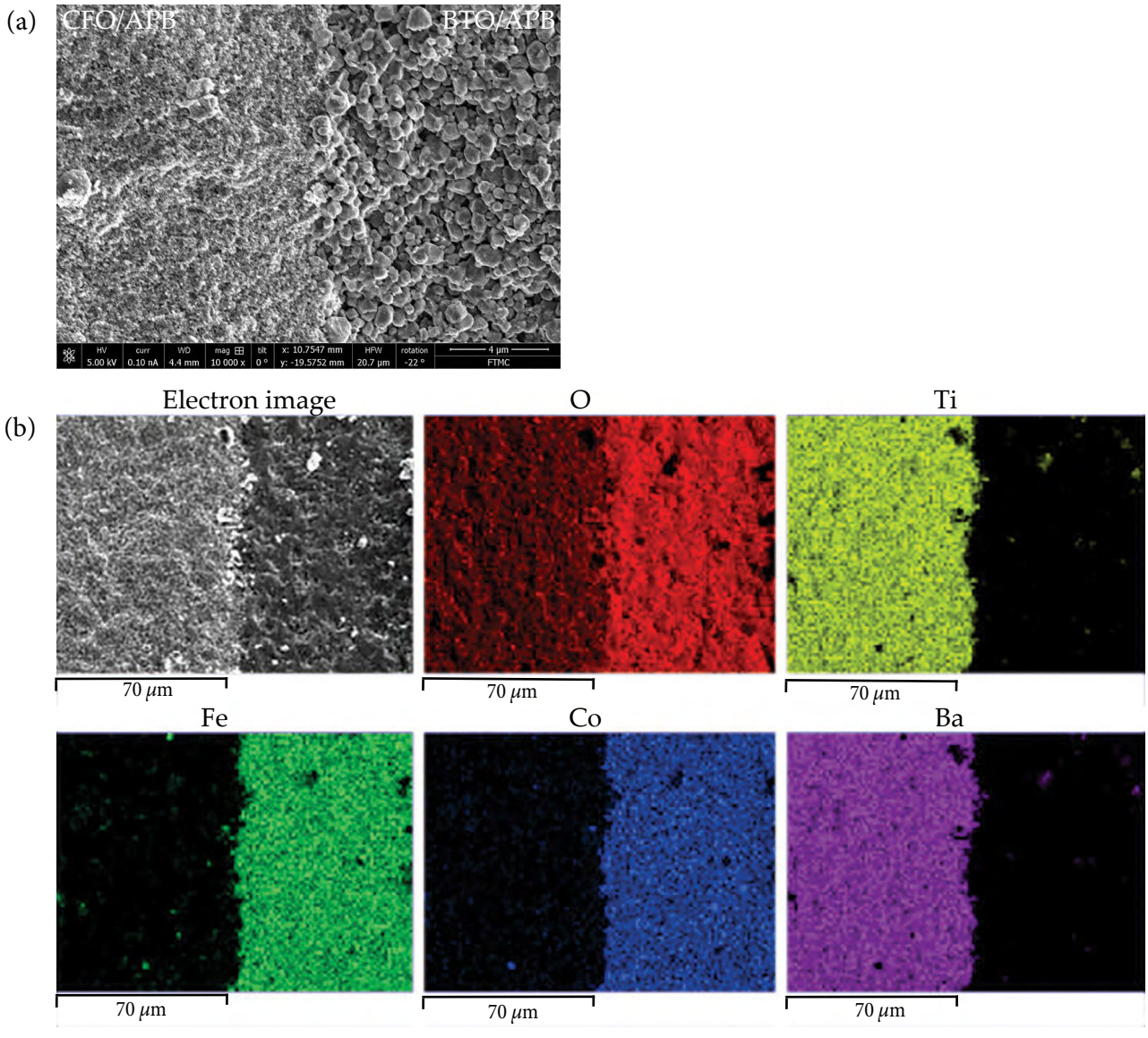

Fig. 2. Scanning electron microscopy of the interface of the CFO and BTO layers (a). Elemental mapping of the interface of the CFO and BTO layers (b). Here the orientation of the layers is opposite.

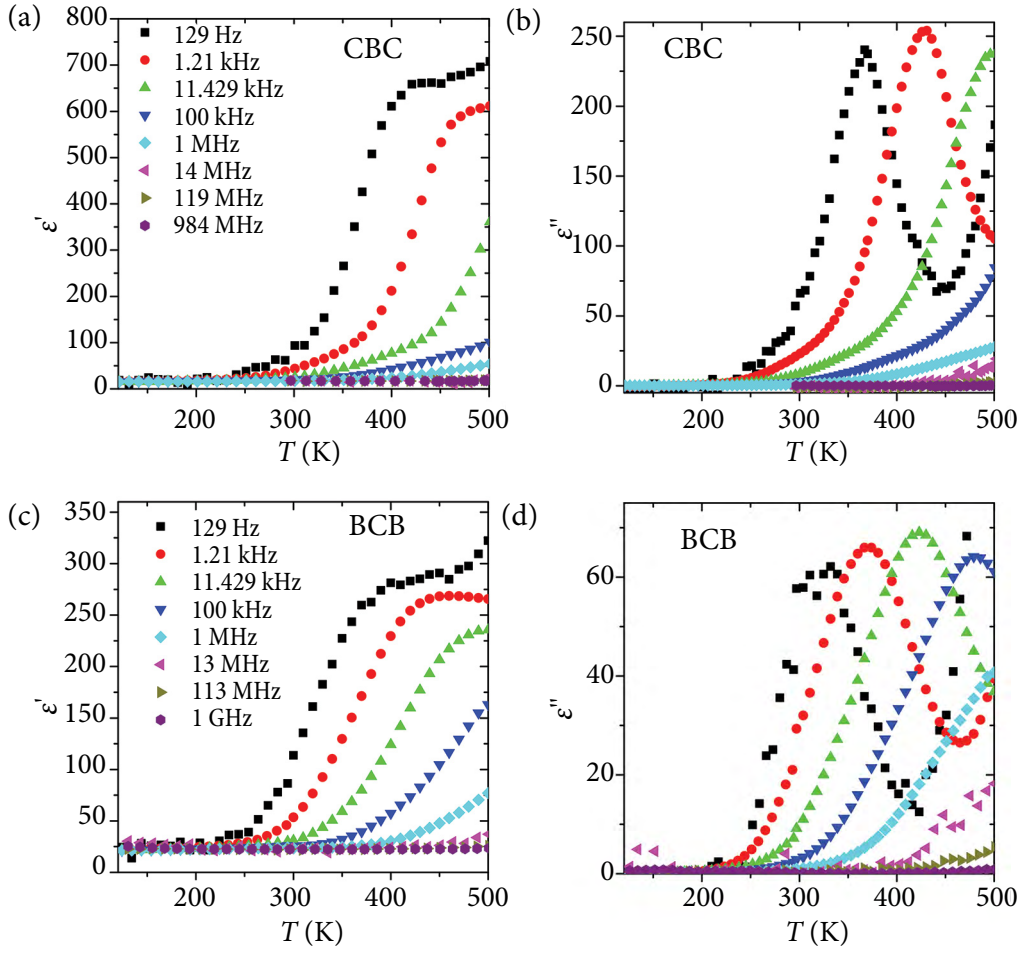

Fig. 3. Temperature dependences of the the real (a) and (c) and imaginary (b) and (d) parts of the dielectric permittivity of layered structures.

anomalies related to the phase transition of $BaTiO_3$ were not detected.

Such behaviour of $\varepsilon(T)$ is determined by very different dielectric properties of $BaTiO_3$ and $CoFe_2O_4$. Cobalt ferrite demonstrates a low dielectric permittivity at room temperature and below it; however, both real and imaginary ε increase rapidly upon heating [18]. In the ferroelectric phase, barium titanate has a higher permittivity but it decreases according to the Curie's law above the phase transition [19].

The frequency spectra of dielectric permittivity demonstrate several relaxation maxima of the imaginary part for both of the samples under investigation, as presented in Fig. 4. The Havriliak–Negami function with $N = 2$ or 3 relaxation terms was used to describe the frequency spectra of ε,

$$\varepsilon = \varepsilon_\infty + \sum_{i=1}^{N} \frac{\Delta\varepsilon_i}{[1+(\mathrm{j}\omega\tau_i)^{1-\alpha_i}]^{\beta_i}}, \qquad (1)$$

where $\varepsilon_\infty = \lim_{\nu\to\infty} \varepsilon$, τ_i is the relaxation time of the ith process, $\omega = 2\pi\nu$ is the angular frequency, α_i and β_i ($0 < \alpha, \beta \leq 1$) describe the broadness and symmetry of the maximum of the imaginary part, and $\mathrm{j}^2 = -1$. The function of two relaxation terms was used for BCB and 3 for CBC spectra. The relaxation time τ depends on the temperature following the Arrhenius law (see Fig. 5). The activation energies are 0.60 eV for BCB and 0.58 for CBC structures which is close to the values obtained for the bulk composites [15].

The Maxwell–Wagner relaxations are related with non-homogeneous media. The difference in the dielectric properties of components leads to the polarization at the interfaces in the external electric field. Such relaxation is typical of the bulk $BaTiO_3$–$CoFe_2O_4$ composites [15]. In the previous case, the polarization occurred on BT/CF and BT/phosphate grain boundaries. But in the studied case, the layered sandwich structure of the sample plays the main role. That can be proved as follows.

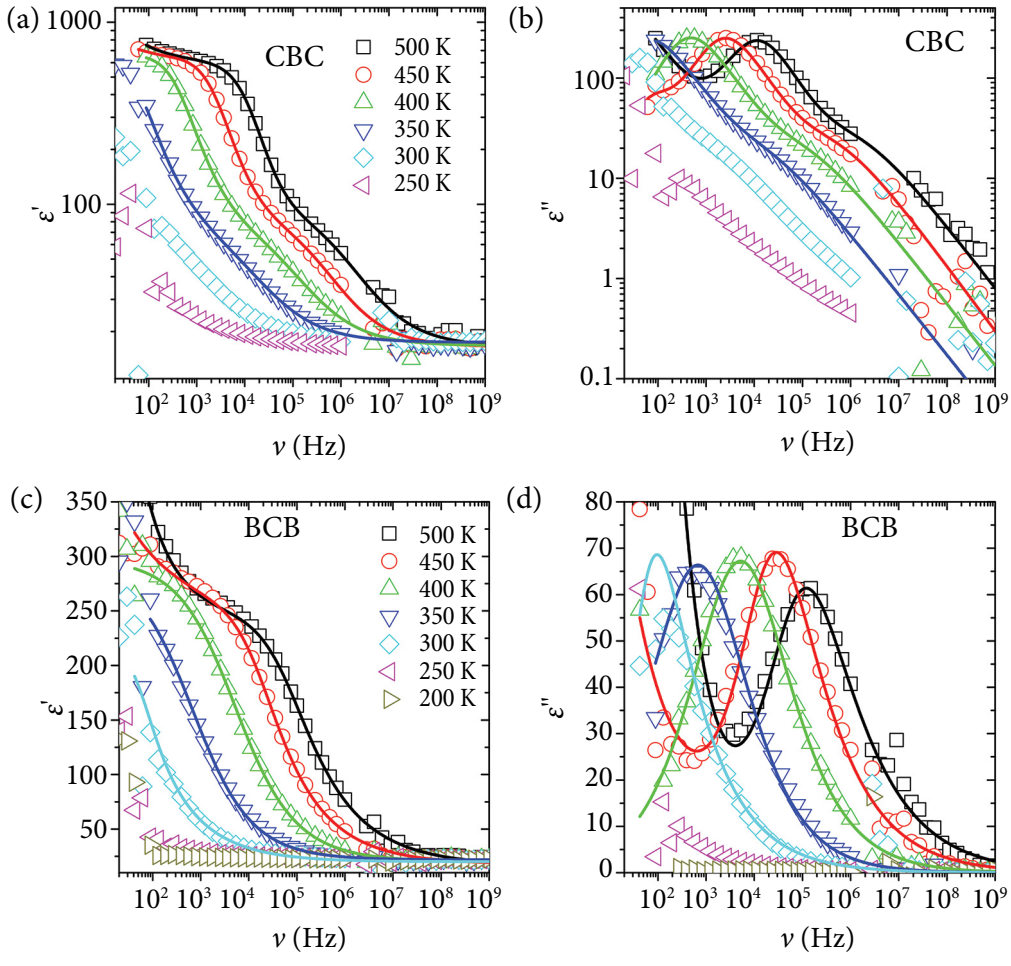

Fig. 4. Frequency dependences of the the real (a) and (c) and imaginary (b) and (d) parts of the dielectric permittivity of layered structures. Symbols stand for the measured data, and lines are the best fits with Eq. (1).

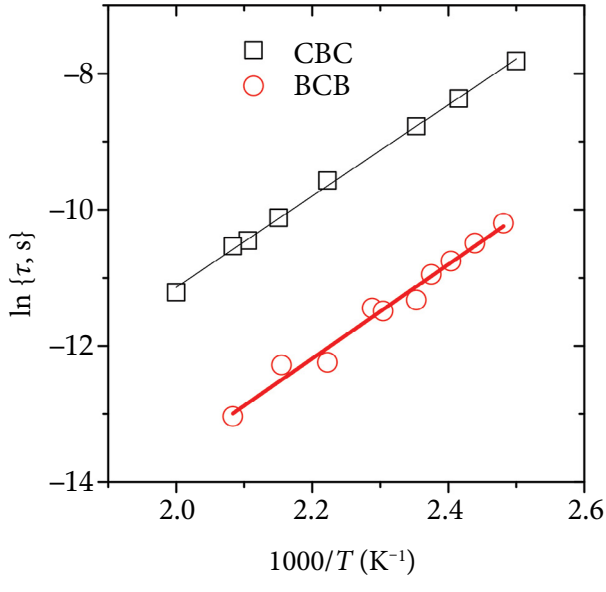

Fig. 5. Temperature dependences of the relaxation time. Symbols stand for the measured data, and lines are the best fits with the Arrhenius law.

The weight concentration of cobalt ferrite in the CBC sample is 66 wt.% and 33 wt.% in BCB. For comparison, the relaxation of the bulk sample of similar compositions $BaTiO_3$–$0.3CoFe_2O_4$ or $BaTiO_3$–$0.6CoFe_2O_4$ is weak and can be observed only in the reciprocal permittivity (electric modulus) spectra. The sample can be considered as a circuit of impedances connected in series and the polarization at the interface between the BT and CF layers is much stronger in comparison to the one at grain boundaries in the bulk composite.

3.2. Magnetization and magnetoelectric coupling

Magnetic hysteresis loops are presented in Fig. 6. The coercive field of the studied samples is as high as 2256 Oe for CBC and 2332 Oe for BCB. That is attributed to the 30 nm size of $CoFe_2O_4$ grains [20]. The saturation magnetization depends on

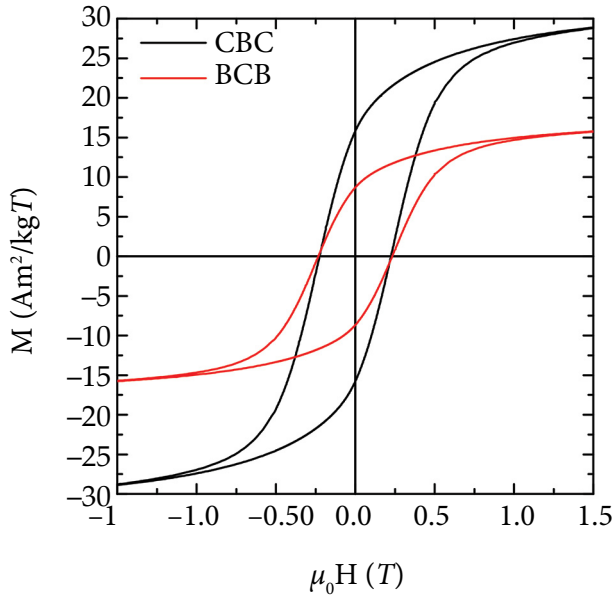

Fig. 6. *M–H* hysteresis loops measured at room temperature.

the concentration of $CoFe_2O_4$ and increases from 17 Am^2/kg for BCB to 31 A m^2/kg for CBC.

The amplitude of the direct magnetoelectric coupling coefficient is presented in Fig. 7. The frequency of the applied H_{ac} field is 90 Hz. The magnetoelectric coefficient of BCB structure reaches 0.2 $mVOe^{-1}cm^{-1}$, and 0.12 $mVOe^{-1}cm^{-1}$ for CBC. Similarly to the bulk composites, the magnetic field dependence reaches a maximum of the coupling coefficient at a field of 0.5 T. That is the size-related effect of the $CoFe_2O_4$ grains of 30 nm [20]. The magnetoelectric coupling of 0.2 $mVOe^{-1}cm^{-1}$ for the BCB structure is higher than that of CBC. The response of both structures is lower in comparison to 1.1 $mVOe^{-1}cm^{-1}$ of bulk phosphate bonded composites [15]. Several factors are responsible for such drawbacks. The main one is the porosity of the samples. Due to this, the magnetostriction effect of the whole CFO layer is lower in comparison to that of sintered ceramics of high density. The mechanical contact between CFO and BTO also loses quality, and finally, being porous, the BTO layer provides a lower piezo voltage.

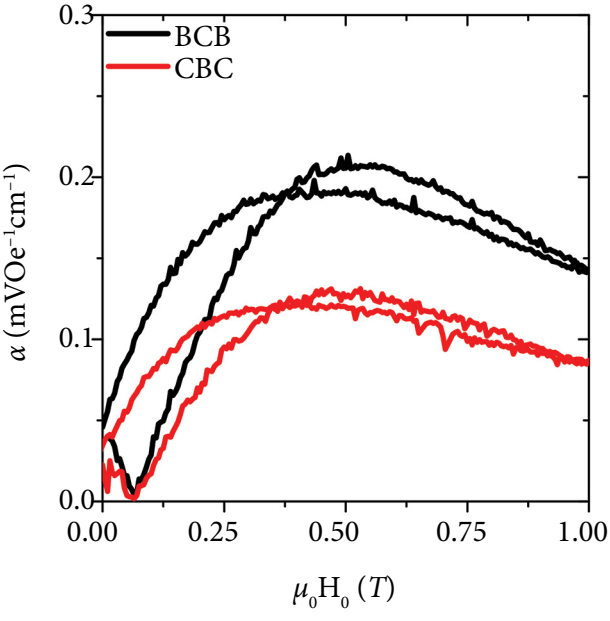

Fig. 7. Amplitude of the magnetoelectric coupling coefficient for the layered structures.

Table 1. Comparison of the direct magnetoelectric coupling coefficients of layered BT-CF structures.

α, $mVOe^{-1}cm^{-1}$	Method	Reference
12	pulse laser deposition	[22]
14	casting + spark plasma sintering	[23]
14×10^{-3}	spin coating	[24]
8.1×10^{-3}	tape casting	[11]
36×10^{-3}	tape casting	[25]
3.9	electrophoretic deposition	[26]

The phosphate binder partially absorbs mechanical stresses and influences the properties of composites [21]. Another factor is that the ferroelectric layer is insulated or separated with CFO. Due to this, it is difficult to polarize it fully.

However, the presence of magnetoelectric coupling evidences the direct interface contact between the phases. That makes the phosphate bonded ceramic-based approach promising for the layered 2–2 structures. The comparison with data presented in the literature (see Table 1) supports the conclusion.

4. Conclusions

The barium titanate and cobalt ferrite powders were bonded with a small amount of aluminium phosphate binder into layered $BaTiO_3$–$CoFe_2O_4$–$BaTiO_3$ and $CoFe_2O_4$–$BaTiO_3$–$CoFe_2O_4$ structures. The dielectric properties were studied in wide temperature and frequency ranges. The behaviour of ε is mostly determined by the layered structure of samples. Huge Maxwell–Wagner relaxations resulting

from the polarization at the interface of layers were observed. Experimentally measured direct magnetoelectric coupling coefficients are 0.2 $mVOe^{-1}cm^{-1}$ for the BCB sample and 0.12 $mVOe^{-1}cm^{-1}$ for CBC. These moderate values are attributed to porosity and difficulties with the polarization of $BaTiO_3$.

The obtained results demonstrate that the proposed approach is promising for the synthesis of the layered structures and may successfully compete with others due to its simplicity. The method is eco-friendly and cost-effective.

Acknowledgements

This work was funded by the Lithuanian Academy of Sciences, Grant No. CERN-VU-2021-2022.

References

[1] G. Liu, C.-W. Nan, Z. Xu, and H. Chen, Coupling interaction in multiferroic $BaTiO_3$–$CoFe_2O_4$ nanostructures, J. Phys. D Appl. Phys. **38**(14), 2321 (2005).

[2] Z. Chu, H. Shi, W. Shi, G. Liu, J. Wu, J. Yang, and S. Dong, Enhanced resonance magnetoelectric coupling in (1-1) connectivity composites, Adv. Mater. **29**(19), 1606022 (2017).

[3] S. Mohan and P. Joy, Magnetic properties of sintered $CoFe_2O_4$–$BaTiO_3$ particulate magnetoelectric composites, Ceram. Int. **45**(9), 12307–12311 (2019).

[4] D. Ghosh, H. Han, J.C. Nino, G. Subhash, and J.L. Jones, Synthesis of $BaTiO_3$-20wt%$CoFe_2O_4$ nanocomposites via spark plasma sintering, J. Am. Ceram. Soc. **95**(8), 2504–2509 (2012).

[5] J. Ma, J. Hu, Z. Li, and C.-W. Nan, Recent progress in multiferroic magnetoelectric composites: from bulk to thin films, Adv. Mater. **23**(9), 1062–1087 (2011).

[6] J.-P. Zhou, H.-C. He, Z. Shi, G. Liu, and C.-W. Nan, Dielectric, magnetic, and magnetoelectric properties of laminated $PbZr_{0.52}Ti_{0.48}O_3$/$CoFe_2O_4$ composite ceramics, J. Appl. Phys. **100**(9), 094106 (2006).

[7] H. Yang, G. Zhang, and Y. Lin, Enhanced magnetoelectric properties of the laminated $BaTiO_3$/$CoFe_2O_4$ composites, J. Alloys Compd. **644**, 390–397 (2015).

[8] R.C. Kambale, D.-Y. Jeong, and J. Ryu, Current status of magnetoelectric composite thin/thick films, Adv. Condens. Matter Phys. **2012**, 824643 (2012).

[9] J.P. Praveen, V.R. Monaji, E. Chandrakala, S. Indla, S. Dinesh Kumar, V. Subramanian, and D. Das, Enhanced magnetoelectric coupling in Ti and Ce substituted lead free CFO-BCZT laminate composites, J. Alloys Compd. **750**, 392–400 (2018).

[10] D. Patil, J.-H. Kim, Y.S. Chai, J.-H. Nam, J.-H. Cho, B.-I. Kim, and K.H. Kim, Large longitudinal magnetoelectric coupling in $NiFe_2O_4$–$BaTiO_3$ laminates, Appl. Phys. Express **4**(7), 073001 (2011).

[11] L. Hao, D. Zhou, Q. Fu, and Y. Hu, Multiferroic properties of multilayered $BaTiO_3$–$CoFe_2O_4$ composites via tape casting method, J. Mater. Sci. **48**(1), 178–185 (2013).

[12] T. Walther, N. Quandt, R. Köferstein, R. Roth, M. Steimecke, and S.G. Ebbinghaus, $BaTiO_3$–$CoFe_2O_4$–$BaTiO_3$ trilayer composite thin films prepared by chemical solution deposition, J. Eur. Ceram. Soc. **36**(3), 559–565 (2016).

[13] Q. Yang, W. Zhang, M. Yuan, L. Kang, J. Feng, W. Pan, and J. Ouyang, Preparation and characterization of self-assembled percolative $BaTiO_3$–$CoFe_2O_4$ nanocomposites via magnetron co-sputtering, Sci. Technol. Adv. Mater. **15**(2), 025003 (2014).

[14] M. dos Santos Amarante, M.J. de Morais Santos, J.P.B. Machado, M.H. Lente, and V.L.O. de Brito, Sintering of layered ferrite-$BaTiO_3$ ceramics: Analysis of interfaces and effects of shrinkage mismatch, Process. Appl. Ceram. **16**(2), 134–142 (2022).

[15] A. Plyushch, D. Lewin, A. Sokal, R. Grigalaitis, V. Shvartsman, J. Macutkevič, S. Salamon, H. Wende, K. Lapko, P. Kuzhir, et al., Magnetoelectric coupling in nonsintered bulk $BaTiO_{3-x}CoFe_2O_4$ multiferroic composites, J. Alloys Compd. **917**, 165519 (2022).

[16] M. Etier, V.V. Shvartsman, S. Salamon, Y. Gao, H. Wende, and D.C. Lupascu, The direct and the converse magnetoelectric effect in multiferroic cobalt ferrite–barium titanate ceramic

composites, J. Am. Ceram. Soc. **99**(11), 3623–3631 (2016).

[17] G.V. Duong, R. Groessinger, M. Schoenhart, and D. Bueno-Basques, The lock-in technique for studying magnetoelectric effect, J. Magn. Magn. Mater. **316**(2), 390–393 (2007).

[18] N. Sivakumar, A. Narayanasamy, C. Chinnasamy, and B. Jeyadevan, Influence of thermal annealing on the dielectric properties and electrical relaxation behaviour in nanostructured $CoFe_2O_4$ ferrite, J. Phys. Condens. Matter **19**(38), 386201 (2007).

[19] W. Zhong, P. Zhang, Y. Wang, and T. Ren, Size effect on the dielectric properties of $BaTiO_3$, Ferroelectrics **160**(1), 55–59 (1994).

[20] C. Chinnasamy, M. Senoue, B. Jeyadevan, O. Perales-Perez, K. Shinoda, and K. Tohji, Synthesis of size-controlled cobalt ferrite particles with high coercivity and squareness ratio, J. Colloid Interface Sci. **263**(1), 80–83 (2003).

[21] A. Plyushch, N. Mačiulis, A. Sokal, R. Grigalaitis, J. Macutkevič, A. Kudlash, N. Apanasevich, K. Lapko, A. Selskis, S.A. Maksimenko, et al., $0.7Pb(Mg_{1/3}Nb_{2/3})O_3$-$0.3PbTiO_3$ phosphate composites: dielectric and ferroelectric properties, Materials **14**(17), 5065 (2021).

[22] X. Zhao, R. Cui, and C. Deng, Magnetoelectric properties of three-layered composite thin film fabricated by pulsed laser deposition, Vacuum **200**, 110978 (2022).

[23] A. Guzu, C.E. Ciomaga, M. Airimioaei, L. Padurariu, L.P. Curecheriu, I. Dumitru, F. Gheorghiu, G. Stoian, M. Grigoras, N. Lupu, et al., Functional properties of randomly mixed and layered $BaTiO_3$-$CoFe_2O_4$ ceramic composites close to the percolation limit, J. Alloys Compd. **796**, 55–64 (2019).

[24] B. Yang, Z. Li, Y. Gao, Y. Lin, and C.-W. Nan, Multiferroic properties of $Bi_{3.15}Nd_{0.85}Ti_3O_{12}$–$CoFe_2O_4$ bilayer films derived by a sol–gel processing, J. Alloys Compd. **509**(13), 4608–4612 (2011).

[25] D. Zhou, L. Hao, S. Gong, Q. Fu, F. Xue, and G. Jian, Magnetoelectric effect of the multilayered $CoFe_2O_4$/$BaTiO_3$ composites fabricated by tape casting, J. Mater. Sci. Mater. Electron. **23**(12), 2098–2103 (2012).

[26] D. Zhou, G. Jian, Y. Zheng, S. Gong, and F. Shi, Electrophoretic deposition of $BaTiO_3$/$CoFe_2O_4$ multiferroic composite films, Appl. Surf. Sci. **257**(17), 7621–7626 (2011).

FOSFATAIS SURIŠTI $CoFe_2O_4$ – $BaTiO_3$ SLUOKSNINIAI DARINIAI: DIELEKTRINĖS RELAKSACIJOS IR MAGNETOELEKTRINĖ SĄVEIKA

A. Plyushch [a], D. Lewin [b], P. Ažubalis [a], V. Kalendra [a], A. Sokal [c], R. Grigalaitis [a], V.V. Shvartsman [b], S. Salamon [d], H. Wende [d], A. Selskis [e], K.N. Lapko [c], D.C. Lupascu [b], J. Banys [a]

[a] *Vilniaus universiteto Fizikos fakultetas, Vilnius, Lietuva*

[b] *Duisburgo-Eseno universiteto Medžiagų mokslo institutas ir Nanointegracijos centras, Esenas, Vokietija*

[c] *Nepriklausomi nuo afiliacijos tyrėjai*

[d] *Duisburgo-Eseno universiteto Fizikos fakultetas ir Nanointegracijos centras, Duisburgas, Vokietija*

[e] *Fizinių ir technologijos mokslų centro Medžiagų struktūrinės analizės skyrius, Vilnius, Lietuva*

Santrauka

Daugiasluoksniai fosfatais surišti $CoFe_2O_4$ – $BaTiO_3$ – $CoFe_2O_4$ (CBC) ir $BaTiO_3$ – $CoFe_2O_4$ – $BaTiO_3$ (BCB) dariniai buvo pagaminti presavimo būdu. Dielektrinės savybės ištirtos 20 Hz – 1 GHz dažnių ir 120–500 K temperatūrų intervaluose. CBC ir BCB dariniuose buvo išmatuotos dielektrinės skvarbos vertės, 15–0,17i ir 22–0,04i atitinkamai, kurios nepriklauso nuo dažnio ir temperatūros žemiau 250 K. Aukštesnėse temperatūrose atsiranda stiprioji dispersija, būdinga Maksvelo–Vagnerio relaksacijai. Toks elgesys yra susijęs su 2–2 fazių erdviniu pasiskirstymu. $BaTiO_3$ – $CoFe_2O_4$ – $BaTiO_3$ darinyje buvo išmatuotas magnetoelektrinės sąveikos koeficientas, kurio gauta vertė yra 0,2 $mVOe^{-1}cm^{-1}$.